

Received 31 October 2023

Accepted 14 November 2023

Edited by W. T. A. Harrison, University of Aberdeen, United Kingdom

This article is part of a collection of articles to commemorate the founding of the African Crystallographic Association and the 75th anniversary of the IUCr.

Keywords: crystal structure; benzimidazolone; triazole; C—H···π(ring) interaction; hydrogen bond.

CCDC reference: 2307930

Supporting information: this article has supporting information at journals.iucr.org/e

Synthesis, structure and Hirshfeld surface analysis of 1,3-bis[(1-octyl-1*H*-1,2,3-triazol-4-yl)methyl]-1*H*-benzo[*d*]imidazol-2(3*H*)-one

Mustapha Zouhair,^a Lhoussaine El Ghayati,^a Hanae El Monfalouti,^b Hicham Abchihi,^a Tuncer Hökelek,^c Mazzah Ahmed,^d Joel T. Mague^e and Nada Kheira Sebbar^{f,b*}

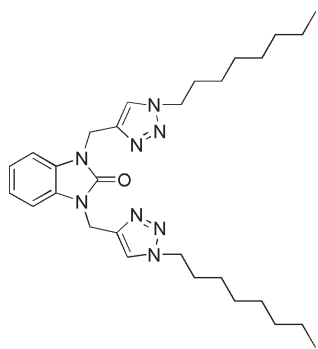
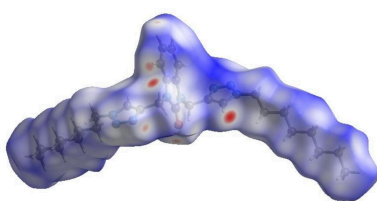
^aLaboratory of Heterocyclic Organic Chemistry, Medicines Science Research Center, Pharmacochemistry Competence Center, Mohammed V University in Rabat, Faculté des Sciences, Av. Ibn Battouta, BP 1014, Rabat, Morocco, ^bLaboratory of Plant Chemistry, Organic and Bioorganic Synthesis, Faculty of Sciences, Mohammed V University in Rabat, 4 Avenue Ibn Battouta, BP 1014 RP, Morocco, ^cDepartment of Physics, Hacettepe University, 06800 Beytepe, Ankara, Türkiye,

^dScience and Technology of Lille USR 3290, Villeneuve d'Ascq cedex, France, ^eDepartment of Chemistry, Tulane University, New Orleans, LA 70118, USA, and ^fLaboratory of Organic and Physical Chemistry, Applied Bioorganic Chemistry Team, Faculty of Sciences, Ibn Zohr University, Agadir, Morocco. *Correspondence e-mail: n.sebbar@uiz.ac.ma

The title molecule, $C_{29}H_{44}N_8O$, adopts a conformation resembling a two-bladed fan with the octyl chains largely in fully extended conformations. In the crystal, C—H···O hydrogen bonds form chains of molecules extending along the *b*-axis direction, which are linked by weak C—H···N hydrogen bonds and C—H···π interactions to generate a three-dimensional network. A Hirshfeld surface analysis of the crystal structure indicates that the most important contributions for the crystal packing are from H···H (68.3%), H···N/N···H (15.7%) and H···C/C···H (10.4%) interactions.

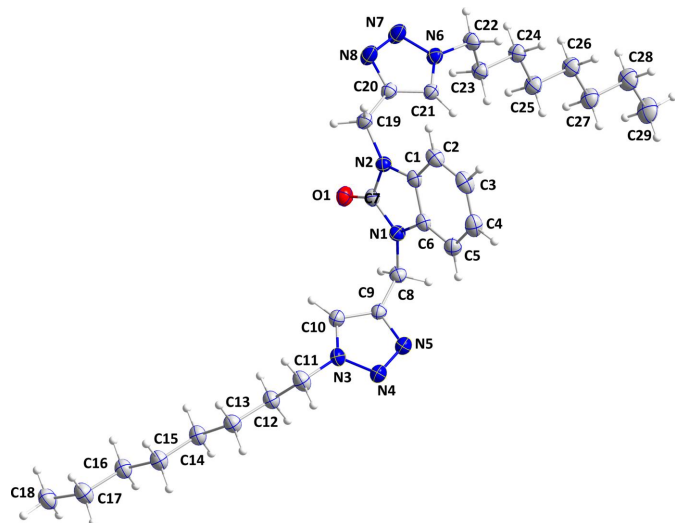
1. Chemical context

Benzimidazolone derivatives display diverse pharmacological and biological properties including antiviral (Ferro *et al.*, 2017), antibacterial (Saber *et al.*, 2020; Menteşe *et al.*, 2021), anticancer (Guillon *et al.*, 2022), anti-Alzheimer's (Mo *et al.*, 2020), antifungal (Ibrahim *et al.*, 2021), and antioxidant (Ibrahim *et al.*, 2021) activities. In our ongoing research in this area, we are synthesizing compounds that combine the 1,2,3-triazole motif with benzimidazol-2-one derivatives. In this report, we present the synthesis and structure of the title compound, $C_{29}H_{44}N_8O$, which was obtained using click chemistry, specifically the copper-catalysed azide–alkyne cycloaddition (CuAAC) method. Additionally, we describe the Hirshfeld surface analysis and calculations on crystal voids and intermolecular interaction energies and energy frameworks.



OPEN ACCESS

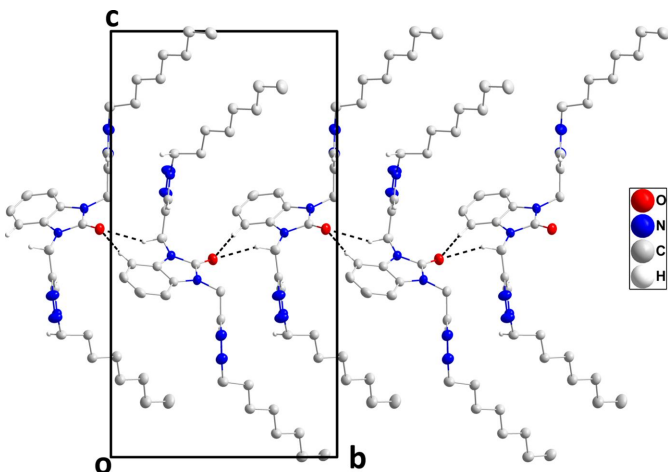
Published under a CC BY 4.0 licence

**Figure 1**

The title molecule with 50% probability ellipsoids.

2. Structural commentary

The title molecule adopts a conformation similar to a two-bladed fan in which the octyltriazolylmethyl substituents extend in opposite directions from the benzimidazolone core (Fig. 1). The C1–C7/N1/N2 benzimidazole moiety is planar to within 0.0155 (13) Å (r.m.s. deviation = 0.007 Å) and the mean planes of the C9/C10/N3–N5 and C20/C21/N6–N8 rings are inclined to the above plane by 75.72 (6) and 83.07 (6)°, respectively; the dihedral angle between the pendant heterocyclic rings is 7.37 (11)°. Both octyl chains have a modest kink near the triazole ring as indicated by the C11–C12–C13–C14 and C22–C23–C24–C25 torsion angles of 169.67 (17) and 168.59 (16)°, respectively. Otherwise, both are in fully extended conformations with the remaining torsion angles differing by no more than about 4° from $\pm 180^\circ$ (Fig. 1).

**Figure 2**

A portion of one chain of molecules viewed along the a -axis direction with $C-H\cdots O$ hydrogen bonds depicted by dashed lines and non-interacting hydrogen atoms omitted for clarity.

Table 1

Hydrogen-bond geometry (\AA , $^\circ$).

$Cg2$ is the centroid of the N3–N5/C9/C10 ring.

$D-H\cdots A$	$D-H$	$H\cdots A$	$D\cdots A$	$D-H\cdots A$
$C2-H2\cdots O1^i$	0.95	2.59	3.502 (2)	162
$C10-H10\cdots N5^{ii}$	0.95	2.44	3.317 (2)	153
$C19-H19A\cdots O1^i$	0.99	2.43	3.334 (2)	152
$C21-H21\cdots N8^{iii}$	0.95	2.62	3.372 (2)	137
$C22-H22A\cdots Cg2^{iv}$	0.99	2.89	3.664 (2)	135

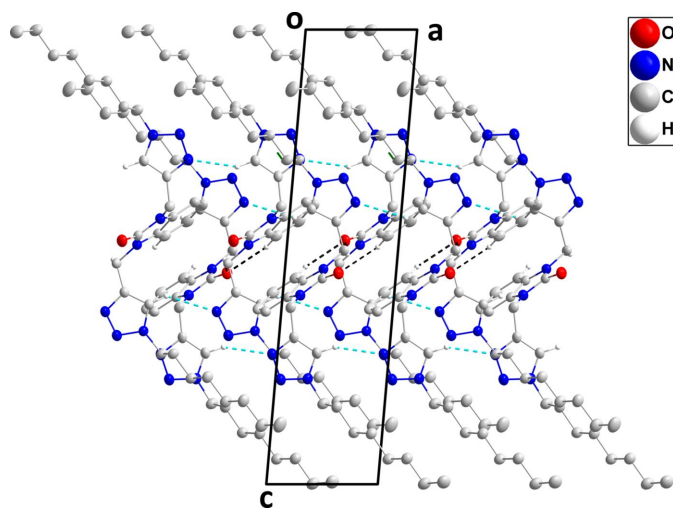
Symmetry codes: (i) $-x + 1, y - \frac{1}{2}, -z + 1$; (ii) $x - 1, y, z$; (iii) $x + 1, y, z$; (iv) $-x + 2, y - \frac{1}{2}, -z + 1$.

3. Supramolecular features

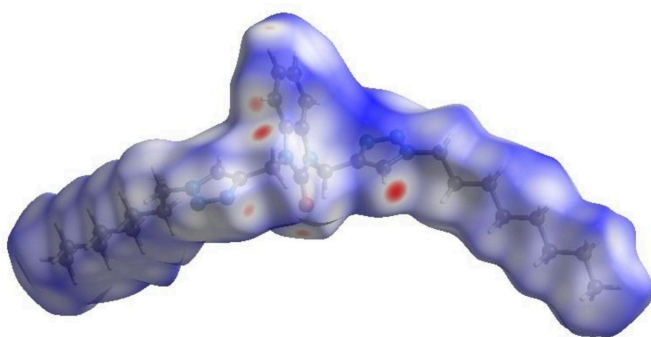
In the crystal, $C2-H2\cdots O1$ and $C19-H19A\cdots O1$ hydrogen bonds (Table 1) form chains of molecules extending along the b -axis direction (Fig. 2). The chains are cross-linked by weak $C10-H10\cdots N5$ and $C21-H21\cdots N8$ hydrogen bonds and by $C22-H22A\cdots Cg2$ interactions (Table 1) into a three-dimensional network (Fig. 3).

4. Hirshfeld surface analysis and computational chemistry

In order to further visualize the intermolecular interactions in the crystal of the title compound, a Hirshfeld surface (HS) analysis was carried out by using *Crystal Explorer 17.5* (Turner *et al.*, 2017), as shown in Fig. 4. The overall two-dimensional fingerprint plot, Fig. 5*a*, and those delineated into $H\cdots H$, $H\cdots N/N\cdots H$, $H\cdots C/C\cdots H$, $H\cdots O/O\cdots H$, $C\cdots N/N\cdots C$ and $N\cdots N$ (McKinnon *et al.*, 2007) are illustrated in Fig. 5*b-g* respectively, together with their relative contributions to the Hirshfeld surface. The most important interaction is $H\cdots H$, contributing 68.3% to the overall crystal packing, which is reflected in Fig. 7*b* as widely scattered points of high density, due to the large hydrogen content of the molecule, with the tip

**Figure 3**

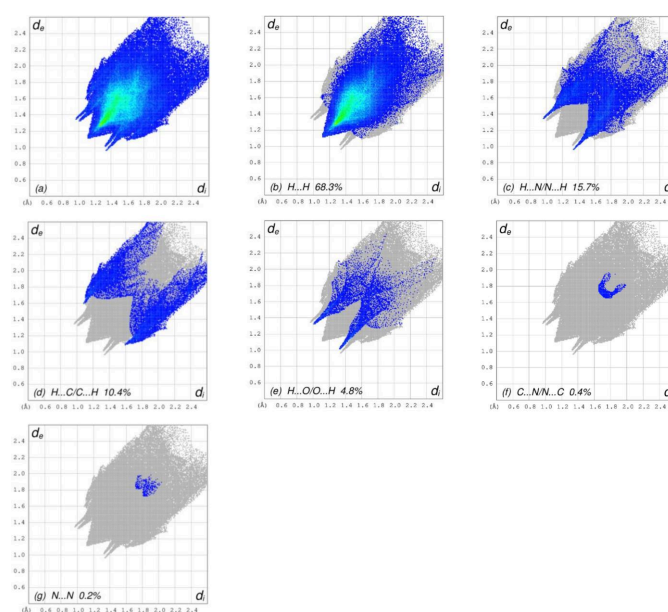
Packing viewed along the b -axis direction with $C-H\cdots O$ and $C-H\cdots N$ hydrogen bonds depicted, respectively, by black and light-blue dashed lines. The $C-H\cdots\pi(\text{ring})$ interactions are depicted by dark-green dashed lines and non-interacting hydrogen atoms omitted for clarity.

**Figure 4**

View of the three-dimensional Hirshfeld surface of the title compound plotted over d_{norm} in the range -0.24 to 1.57 a.u.

at $d_e = d_i = 1.12$ Å. The pair of characteristic wings in the fingerprint plot delineated into H···N/N···H contacts (15.7% contribution to the HS; Fig. 5c) is viewed as pair of spikes with the tips at $d_e + d_i = 2.30$ Å. In the presence of C–H···π interactions, the H···C/C···H contacts, contributing 10.4% to the overall crystal packing, are reflected in Fig. 5d with the tips at $d_e + d_i = 2.69$ Å. The pair of characteristic wings in the fingerprint plot delineated into H···O/O···H contacts (4.8% contribution to the HS; Fig. 5e) is viewed as pair of spikes with the tips at $d_e + d_i = 2.32$ Å. Finally, the C···N/N···C (Fig. 5f) and N···N (Fig. 5g) contacts, with 0.4% and 0.2% contributions, respectively, to the HS, have very low distributions of points.

A void analysis was performed by summing the electron densities of the spherically symmetric atoms contained in the

**Figure 5**

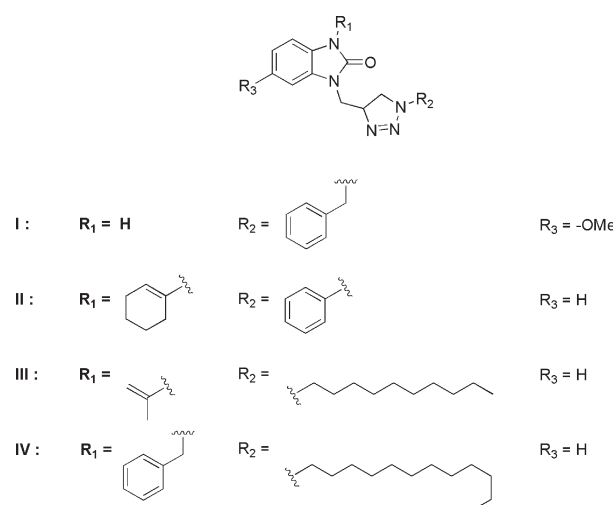
The full two-dimensional fingerprint plots for the title compound, showing (a) all interactions, and delineated into (b) H···H, (c) H···N/N···H, (d) H···C/C···H, (e) H···O/O···H, (f) C···N/N···C and (g) N···N interactions. The d_i and d_e values are the closest internal and external distances (in Å) from given points on the Hirshfeld surface.

asymmetric unit (Turner *et al.*, 2011). The void surface is defined as an isosurface of the procrystal electron density and is calculated for the whole unit cell where the void surface meets the boundary of the unit cell and capping faces are generated to create an enclosed volume. The volume of the crystal voids (supplementary Fig. S1) and the percentage of free space in the unit cell are calculated to be 198.6 and 13.4 Å³, respectively.

The intermolecular interaction energies were calculated using the CE-B3LYP/6-31G(d,p) energy model available in *Crystal Explorer* 17.5 (Turner *et al.*, 2017). The total intermolecular energy (E_{tot}) is the sum of electrostatic (E_{ele}), polarization (E_{pol}), dispersion (E_{dis}) and exchange–repulsion (E_{rep}) energies (Turner *et al.*, 2015) with scale factors of 1.057, 0.740, 0.871 and 0.618, respectively (Mackenzie *et al.*, 2017). Energy frameworks were constructed for E_{ele} (red cylinders), E_{dis} (green cylinders) and E_{tot} (blue cylinders) (supplementary Fig. 2a and 2b). These data indicate that dispersion energy is the most important contributor to the cohesion of the crystal structure of the title compound. The theoretical optimization of the title structure in the gas phase was conducted by density functional theory (DFT), using the standard B3LYP functional and 6-311 G(d,p) basis-set calculations (Becke, 1993). The energy band gap [$\Delta E = E_{\text{LUMO}} - E_{\text{HOMO}}$] of the molecule is 5.04 eV, and the frontier molecular orbitals, E_{HOMO} and E_{LUMO} have relative energies of -5.72 and 0.68 eV, respectively (supplementary Tables 1 and 2 and supplementary Fig. S3).

5. Database survey

A survey of the Cambridge Structural Database (CSD, Version 5.42, last update February 2023; Groom *et al.*, 2016) for structures similar to the title molecule gave hits for compound **I** with $R_1 = \text{H}$, $R_2 = -\text{CH}_2\text{C}_6\text{H}_5$ and $R_3 = -\text{OCH}_3$ (CSD refcode HIJXAC; El Bakri *et al.*, 2018), **II** with $R_1 = -\text{C}_6\text{H}_9$, $R_2 = -\text{C}_6\text{H}_5$ and $R_3 = -\text{H}$ (PAZFOO; Adardour *et al.*, 2017), **III** with $R_1 = -\text{C}(\text{CH}_3)=\text{CH}_2$, $R_2 = -\text{C}_{10}\text{H}_{22}$ and $R_3 = -\text{H}$ (ETAJOB; Saber *et al.*, 2021) and **IV** with $R_1 = -\text{CH}_2\text{C}_6\text{H}_5$, $R_2 = -\text{C}_{12}\text{H}_{26}$ and $R_3 = -\text{H}$ (ETAKAO; Saber *et al.*, 2021).



6. Synthesis and crystallization

To a solution of 1.64 mmol of 1,3-di(prop-2-ynyl)-1*H*-benzimidazol-2-one and 2 mmol of 1-azidoctane in 15 ml of ethanol were added 1.15 mmol of CuSO₄ and 2.62 mmol of sodium ascorbate dissolved in 10 ml of distilled water. The reaction mixture was stirred for 10 h at room temperature and monitored by TLC. After filtration and concentration of the solution under reduced pressure, the residue obtained was chromatographed on a silica gel column using ethyl acetate/hexane (3/1) as eluent. Colourless plates of the title compound in 73% yield were recrystallized from ethanol solution.

7. Refinement

Crystal data, data collection and structure refinement details are summarized in Table 2. H atoms were positioned with idealized geometry (C—H = 0.95–0.99 Å) and refined isotropically with $U_{\text{iso}}(\text{H}) = 1.2\text{--}1.5U_{\text{eq}}(\text{C})$ using a riding model.

Funding information

JTM thanks Tulane University for support of the Tulane Crystallography Laboratory. TH is grateful to Hacettepe University Scientific Research Project Unit (grant No. 013 D04 602 004).

References

- Adardour, M., Loughzail, M., Dahaoui, S., Baouid, A. & Berraho, M. (2017). *IUCrData*, **2**, x170907.
- Becke, A. D. (1993). *J. Chem. Phys.* **98**, 5648–5652.
- Brandenburg, K. & Putz, H. (2012). *DIAMOND*. Crystal Impact GbR, Bonn, Germany.
- Bruker (2020). *APEX3* and *SAINT*. Bruker AXS LLC, Madison, Wisconsin, USA.
- El Bakri, Y., Lai, C. H., Sebhaoui, J., Ali, A. B., Ramli, Y., Essassi, E. M. & Mague, J. T. (2018). *DATACC*, **17**, 472–482.
- Ferro, S., Buemi, M. R., De Luca, L., Agharbaoui, F. E., Pannecouque, C. & Monforte, A. M. (2017). *Bioorg. Med. Chem.* **25**, 3861–3870.
- Groom, C. R., Bruno, I. J., Lightfoot, M. P. & Ward, S. C. (2016). *Acta Cryst. B* **72**, 171–179.
- Guillon, J., Savrimoutou, S., Albenque-Rubio, S., Pinaud, N., Moreau, S. & Desplat, V. (2022). *Molbank*, M1333.
- Ibrahim, S., Ghabi, A., Amiri, N., Mtiraoui, H., Hajji, M., Bel-Hadj-Tahar, R. & Msaddek, M. (2021). *Monatsh. Chem.* **152**, 523–535.
- Krause, L., Herbst-Irmer, R., Sheldrick, G. M. & Stalke, D. (2015). *J. Appl. Cryst.* **48**, 3–10.
- Mackenzie, C. F., Spackman, P. R., Jayatilaka, D. & Spackman, M. A. (2017). *IUCrJ*, **4**, 575–587.
- McKinnon, J. J., Jayatilaka, D. & Spackman, M. A. (2007). *Chem. Commun.* 3814–3816.
- Menteşe, E., Güven, O., Çalışkan, N. & Baltaş, N. (2021). *J. Heterocycl. Chem.* **58**, 1259–1267.
- Mo, J., Chen, T., Yang, H., Guo, Y., Li, Q., Qiao, Y., Lin, H., Feng, F., Liu, W., Chen, Y., Liu, Z. & Sun, H. (2020). *J. Enzyme Inhib. Med. Chem.* **35**, 330–343.
- Saber, A., Anouar, E. H., Sebbar, G., Ibrahim, B. E., Srhir, M., Hökelek, T., Mague, J. T., Ghayati, L. E., Sebbar, N. K. & Essassi, E. M. (2021). *J. Mol. Struct.* **1242**, 130719.
- Saber, A., Sebbar, N. K., Sert, Y., Alzaqri, N., Hökelek, T., El Ghayati, L., Talbaoui, A., Mague, J. T., Baba, Y. F., Urrutigoity, M. & Essassi, E. M. (2020). *J. Mol. Struct.* **1200**, 127174.
- Sheldrick, G. M. (2008). *Acta Cryst. A* **64**, 112–122.
- Sheldrick, G. M. (2015a). *Acta Cryst. A* **71**, 3–8.
- Sheldrick, G. M. (2015b). *Acta Cryst. C* **71**, 3–8.
- Turner, M. J., McKinnon, J. J., Jayatilaka, D. & Spackman, M. A. (2011). *CrystEngComm*, **13**, 1804–1813.
- Turner, M. J., McKinnon, J. J., Wolff, S. K., Grimwood, D. J., Spackman, P. R., Jayatilaka, D. & Spackman, M. A. (2017). *CrystalExplorer17*. The University of Western Australia.
- Turner, M. J., Thomas, S. P., Shi, M. W., Jayatilaka, D. & Spackman, M. A. (2015). *Chem. Commun.* **51**, 3735–3738.

Table 2
Experimental details.

Crystal data	
Chemical formula	C ₂₉ H ₄₄ N ₈ O
M_r	520.72
Crystal system, space group	Monoclinic, <i>P</i> 2 ₁
Temperature (K)	150
a, b, c (Å)	5.5229 (2), 11.9579 (5), 22.5767 (9)
β (°)	94.962 (1)
V (Å ³)	1485.43 (10)
Z	2
Radiation type	Mo $K\alpha$
μ (mm ⁻¹)	0.07
Crystal size (mm)	0.43 × 0.24 × 0.04
Data collection	
Diffractometer	Bruker D8 QUEST PHOTON 3 diffractometer
Absorption correction	Numerical (<i>SADABS</i> ; Krause <i>et al.</i> , 2015)
T_{\min}, T_{\max}	0.97, 1.00
No. of measured, independent and observed [$I > 2\sigma(I)$] reflections	44175, 7403, 6607
R_{int}	0.040
(sin θ/λ) _{max} (Å ⁻¹)	0.668
Refinement	
$R[F^2 > 2\sigma(F^2)]$, $wR(F^2)$, S	0.036, 0.090, 1.05
No. of reflections	7403
No. of parameters	346
No. of restraints	1
H-atom treatment	H-atom parameters constrained
$\Delta\rho_{\text{max}}, \Delta\rho_{\text{min}}$ (e Å ⁻³)	0.21, -0.15
Absolute structure	Refined as an inversion twin
Absolute structure parameter	0.2 (13)

Computer programs: *APEX3* and *SAINT* (Bruker, 2020), *SHELXT* (Sheldrick, 2015a), *SHELXL2018/1* (Sheldrick, 2015b), *DIAMOND* (Brandenburg & Putz, 2012) and *SHELXTL* (Sheldrick, 2008).

supporting information

Acta Cryst. (2023). E79, 1179-1182 [https://doi.org/10.1107/S2056989023009891]

Synthesis, structure and Hirshfeld surface analysis of 1,3-bis[(1-octyl-1*H*-1,2,3-triazol-4-yl)methyl]-1*H*-benzo[*d*]imidazol-2(3*H*)-one

Mustapha Zouhair, Lhoussaine El Ghayati, Hanae El Monfalouti, Hicham Abchihi, Tuncer Hökelek, Mazzah Ahmed, Joel T. Mague and Nada Kheira Sebbar

Computing details

1,3-Bis[(1-octyl-1*H*-1,2,3-triazol-4-yl)methyl]-1*H*-benzo[*d*]imidazol-2(3*H*)-one

Crystal data

C₂₉H₄₄N₈O
 $M_r = 520.72$
Monoclinic, $P2_1$
 $a = 5.5229$ (2) Å
 $b = 11.9579$ (5) Å
 $c = 22.5767$ (9) Å
 $\beta = 94.962$ (1)°
 $V = 1485.43$ (10) Å³
 $Z = 2$

$F(000) = 564$
 $D_x = 1.164 \text{ Mg m}^{-3}$
Mo $K\alpha$ radiation, $\lambda = 0.71073$ Å
Cell parameters from 9942 reflections
 $\theta = 2.5\text{--}28.3^\circ$
 $\mu = 0.07 \text{ mm}^{-1}$
 $T = 150 \text{ K}$
Plate, colourless
0.43 × 0.24 × 0.04 mm

Data collection

Bruker D8 QUEST PHOTON 3
diffractometer
Radiation source: fine-focus sealed tube
Graphite monochromator
Detector resolution: 7.3910 pixels mm⁻¹
 φ and ω scans
Absorption correction: numerical
(SADABS; Krause *et al.*, 2015)
 $T_{\min} = 0.97$, $T_{\max} = 1.00$

44175 measured reflections
7403 independent reflections
6607 reflections with $I > 2\sigma(I)$
 $R_{\text{int}} = 0.040$
 $\theta_{\max} = 28.3^\circ$, $\theta_{\min} = 1.8^\circ$
 $h = -7 \rightarrow 7$
 $k = -15 \rightarrow 15$
 $l = -30 \rightarrow 30$

Refinement

Refinement on F^2
Least-squares matrix: full
 $R[F^2 > 2\sigma(F^2)] = 0.036$
 $wR(F^2) = 0.090$
 $S = 1.05$
7403 reflections
346 parameters
1 restraint
Primary atom site location: dual
Secondary atom site location: difference Fourier map

Hydrogen site location: inferred from neighbouring sites
H-atom parameters constrained
 $w = 1/[\sigma^2(F_o^2) + (0.0469P)^2 + 0.1166P]$
where $P = (F_o^2 + 2F_c^2)/3$
 $(\Delta/\sigma)_{\max} < 0.001$
 $\Delta\rho_{\max} = 0.21 \text{ e } \text{\AA}^{-3}$
 $\Delta\rho_{\min} = -0.15 \text{ e } \text{\AA}^{-3}$
Absolute structure: Refined as an inversion twin
Absolute structure parameter: 0.2 (13)

Special details

Experimental. The diffraction data were obtained from 7 sets of frames, each of width 0.5° in ω or φ , collected with scan parameters determined by the "strategy" routine in *APEX3*. The scan time was 25 sec/frame.

Geometry. All esds (except the esd in the dihedral angle between two l.s. planes) are estimated using the full covariance matrix. The cell esds are taken into account individually in the estimation of esds in distances, angles and torsion angles; correlations between esds in cell parameters are only used when they are defined by crystal symmetry. An approximate (isotropic) treatment of cell esds is used for estimating esds involving l.s. planes.

Refinement. Refinement of F^2 against ALL reflections. The weighted R-factor wR and goodness of fit S are based on F^2 , conventional R-factors R are based on F, with F set to zero for negative F^2 . The threshold expression of $F^2 > 2\text{sigma}(F^2)$ is used only for calculating R-factors(gt) etc. and is not relevant to the choice of reflections for refinement. R-factors based on F^2 are statistically about twice as large as those based on F, and R-factors based on ALL data will be even larger. H-atoms attached to carbon were placed in calculated positions ($C-H = 0.95 - 0.99 \text{ \AA}$). All were included as riding contributions with isotropic displacement parameters 1.2 - 1.5 times those of the attached atoms. Refined as a 2-component inversion twin.

Fractional atomic coordinates and isotropic or equivalent isotropic displacement parameters (\AA^2)

	<i>x</i>	<i>y</i>	<i>z</i>	$U_{\text{iso}}^*/U_{\text{eq}}$
O1	0.5165 (2)	0.45034 (11)	0.46448 (6)	0.0329 (3)
N1	0.8422 (3)	0.38162 (12)	0.41592 (6)	0.0266 (3)
N2	0.6546 (3)	0.26610 (12)	0.47315 (6)	0.0256 (3)
N3	0.7105 (3)	0.48912 (14)	0.23204 (7)	0.0308 (3)
N4	0.9528 (3)	0.49012 (15)	0.23032 (7)	0.0357 (4)
N5	1.0483 (3)	0.48764 (14)	0.28579 (7)	0.0343 (4)
N6	0.7789 (3)	0.26119 (13)	0.66306 (6)	0.0276 (3)
N7	0.5441 (3)	0.25415 (17)	0.67279 (7)	0.0402 (4)
N8	0.4205 (3)	0.24210 (16)	0.62051 (7)	0.0377 (4)
C1	0.8325 (3)	0.20418 (14)	0.44791 (8)	0.0261 (4)
C2	0.8978 (4)	0.09248 (15)	0.45373 (9)	0.0316 (4)
H2	0.816702	0.042829	0.478248	0.038*
C3	1.0882 (4)	0.05678 (16)	0.42184 (9)	0.0358 (4)
H3	1.138081	-0.019205	0.424677	0.043*
C4	1.2070 (4)	0.12896 (17)	0.38608 (9)	0.0363 (4)
H4	1.337097	0.101465	0.365294	0.044*
C5	1.1398 (3)	0.24138 (16)	0.37988 (8)	0.0308 (4)
H5	1.219570	0.290810	0.354969	0.037*
C6	0.9523 (3)	0.27692 (14)	0.41167 (7)	0.0256 (3)
C7	0.6557 (3)	0.37503 (15)	0.45279 (7)	0.0255 (3)
C8	0.9182 (3)	0.48505 (15)	0.38886 (8)	0.0286 (4)
H8A	1.094756	0.495617	0.398973	0.034*
H8B	0.832786	0.548675	0.405854	0.034*
C9	0.8673 (3)	0.48614 (15)	0.32269 (8)	0.0269 (3)
C10	0.6497 (3)	0.48710 (16)	0.28838 (8)	0.0304 (4)
H10	0.490916	0.486484	0.301568	0.037*
C11	0.5501 (4)	0.49558 (17)	0.17728 (9)	0.0363 (4)
H11A	0.424118	0.436762	0.177800	0.044*
H11B	0.645578	0.481045	0.142950	0.044*
C12	0.4278 (3)	0.60839 (16)	0.16948 (8)	0.0316 (4)
H12A	0.553863	0.666846	0.167562	0.038*

H12B	0.337533	0.624078	0.204577	0.038*
C13	0.2529 (4)	0.61468 (16)	0.11355 (8)	0.0325 (4)
H13A	0.347180	0.612977	0.078210	0.039*
H13B	0.145729	0.548191	0.111835	0.039*
C14	0.0970 (4)	0.71974 (16)	0.11140 (9)	0.0325 (4)
H14A	0.205307	0.785813	0.114617	0.039*
H14B	0.000482	0.720037	0.146372	0.039*
C15	-0.0758 (4)	0.73133 (16)	0.05545 (9)	0.0340 (4)
H15A	0.020707	0.736967	0.020592	0.041*
H15B	-0.176824	0.663028	0.050563	0.041*
C16	-0.2417 (4)	0.83263 (17)	0.05645 (9)	0.0346 (4)
H16A	-0.140055	0.900797	0.060959	0.042*
H16B	-0.335843	0.827341	0.091726	0.042*
C17	-0.4187 (4)	0.84527 (18)	0.00121 (9)	0.0418 (5)
H17A	-0.325170	0.855305	-0.033890	0.050*
H17B	-0.514793	0.775659	-0.004678	0.050*
C18	-0.5909 (4)	0.9431 (2)	0.00497 (10)	0.0454 (5)
H18A	-0.697235	0.948212	-0.031997	0.068*
H18B	-0.497132	1.012380	0.010853	0.068*
H18C	-0.689828	0.931993	0.038498	0.068*
C19	0.4857 (3)	0.22611 (15)	0.51395 (8)	0.0288 (4)
H19A	0.453376	0.145736	0.506273	0.035*
H19B	0.329889	0.266739	0.506328	0.035*
C20	0.5775 (3)	0.24109 (14)	0.57782 (8)	0.0257 (3)
C21	0.8082 (3)	0.25252 (15)	0.60465 (7)	0.0259 (3)
H21	0.956179	0.254009	0.586136	0.031*
C22	0.9617 (3)	0.28057 (16)	0.71286 (8)	0.0312 (4)
H22A	1.096178	0.226424	0.710619	0.037*
H22B	0.887647	0.267285	0.750639	0.037*
C23	1.0639 (3)	0.39888 (15)	0.71301 (8)	0.0298 (4)
H23A	1.146748	0.411157	0.676381	0.036*
H23B	0.929314	0.453473	0.713353	0.036*
C24	1.2429 (4)	0.41756 (16)	0.76706 (8)	0.0312 (4)
H24A	1.356372	0.353377	0.771095	0.037*
H24B	1.152369	0.419553	0.803024	0.037*
C25	1.3899 (4)	0.52512 (16)	0.76421 (9)	0.0335 (4)
H25A	1.478246	0.524128	0.727887	0.040*
H25B	1.277315	0.589698	0.761315	0.040*
C26	1.5718 (4)	0.54024 (17)	0.81829 (9)	0.0356 (4)
H26A	1.677894	0.473452	0.822144	0.043*
H26B	1.481523	0.544120	0.854257	0.043*
C27	1.7314 (4)	0.64393 (17)	0.81632 (9)	0.0374 (4)
H27A	1.819955	0.641269	0.780050	0.045*
H27B	1.626618	0.711228	0.813756	0.045*
C28	1.9139 (4)	0.65407 (19)	0.87038 (10)	0.0439 (5)
H28A	1.824831	0.657064	0.906555	0.053*
H28B	2.017259	0.586294	0.873072	0.053*
C29	2.0762 (4)	0.7564 (2)	0.86910 (11)	0.0512 (6)

H29A	2.192124	0.756753	0.904500	0.077*
H29B	1.976150	0.824116	0.868607	0.077*
H29C	2.164945	0.754289	0.833362	0.077*

Atomic displacement parameters (\AA^2)

	U^{11}	U^{22}	U^{33}	U^{12}	U^{13}	U^{23}
O1	0.0295 (7)	0.0286 (6)	0.0409 (8)	0.0049 (5)	0.0046 (6)	-0.0024 (6)
N1	0.0274 (7)	0.0221 (7)	0.0306 (8)	0.0014 (6)	0.0041 (6)	0.0023 (6)
N2	0.0252 (7)	0.0233 (7)	0.0284 (7)	-0.0016 (6)	0.0024 (6)	0.0016 (6)
N3	0.0276 (7)	0.0312 (8)	0.0334 (8)	0.0053 (7)	0.0012 (6)	0.0029 (7)
N4	0.0281 (8)	0.0429 (9)	0.0365 (9)	0.0031 (7)	0.0058 (7)	0.0046 (8)
N5	0.0268 (7)	0.0394 (9)	0.0372 (9)	0.0005 (7)	0.0053 (7)	0.0046 (7)
N6	0.0252 (7)	0.0291 (7)	0.0283 (7)	-0.0042 (6)	0.0013 (6)	-0.0016 (6)
N7	0.0272 (8)	0.0605 (11)	0.0331 (8)	-0.0084 (8)	0.0041 (7)	-0.0057 (8)
N8	0.0254 (8)	0.0553 (11)	0.0326 (8)	-0.0058 (7)	0.0043 (6)	-0.0065 (8)
C1	0.0250 (8)	0.0263 (8)	0.0263 (9)	0.0005 (7)	-0.0020 (7)	-0.0012 (7)
C2	0.0370 (10)	0.0240 (8)	0.0325 (10)	-0.0010 (8)	-0.0052 (8)	-0.0006 (7)
C3	0.0426 (11)	0.0261 (9)	0.0370 (11)	0.0072 (8)	-0.0061 (9)	-0.0065 (8)
C4	0.0349 (10)	0.0392 (11)	0.0339 (10)	0.0089 (8)	-0.0013 (8)	-0.0104 (8)
C5	0.0301 (9)	0.0338 (10)	0.0283 (9)	0.0017 (7)	0.0019 (7)	-0.0022 (7)
C6	0.0249 (8)	0.0248 (8)	0.0264 (8)	0.0015 (7)	-0.0024 (7)	-0.0015 (7)
C7	0.0234 (8)	0.0256 (8)	0.0271 (8)	-0.0011 (7)	-0.0011 (7)	-0.0019 (7)
C8	0.0283 (8)	0.0243 (8)	0.0327 (9)	-0.0028 (7)	-0.0002 (7)	0.0021 (7)
C9	0.0230 (8)	0.0234 (7)	0.0344 (9)	0.0002 (7)	0.0038 (7)	0.0051 (7)
C10	0.0250 (8)	0.0331 (9)	0.0335 (9)	0.0020 (8)	0.0043 (7)	0.0038 (8)
C11	0.0380 (10)	0.0366 (10)	0.0332 (10)	0.0079 (9)	-0.0042 (8)	-0.0013 (8)
C12	0.0292 (9)	0.0325 (9)	0.0326 (9)	0.0031 (7)	0.0005 (8)	0.0033 (7)
C13	0.0330 (10)	0.0329 (10)	0.0312 (9)	0.0038 (7)	0.0002 (8)	-0.0001 (7)
C14	0.0315 (9)	0.0312 (9)	0.0341 (10)	0.0027 (8)	-0.0015 (8)	-0.0008 (7)
C15	0.0346 (10)	0.0339 (10)	0.0326 (10)	0.0034 (8)	-0.0019 (8)	-0.0010 (7)
C16	0.0337 (10)	0.0334 (9)	0.0359 (10)	0.0026 (8)	-0.0018 (8)	0.0016 (8)
C17	0.0437 (12)	0.0425 (12)	0.0377 (11)	0.0081 (9)	-0.0052 (9)	0.0032 (9)
C18	0.0457 (12)	0.0443 (12)	0.0452 (13)	0.0109 (10)	-0.0005 (10)	0.0095 (10)
C19	0.0255 (8)	0.0317 (9)	0.0291 (9)	-0.0070 (7)	0.0012 (7)	0.0016 (7)
C20	0.0244 (8)	0.0231 (8)	0.0299 (9)	-0.0015 (6)	0.0033 (7)	-0.0001 (6)
C21	0.0236 (8)	0.0261 (8)	0.0283 (8)	-0.0012 (7)	0.0034 (7)	0.0004 (7)
C22	0.0321 (9)	0.0331 (9)	0.0272 (9)	-0.0068 (8)	-0.0046 (7)	0.0003 (7)
C23	0.0301 (9)	0.0294 (9)	0.0291 (9)	-0.0031 (7)	-0.0019 (7)	-0.0011 (7)
C24	0.0326 (10)	0.0310 (9)	0.0295 (9)	-0.0050 (7)	-0.0010 (8)	-0.0016 (7)
C25	0.0317 (10)	0.0313 (9)	0.0367 (11)	-0.0065 (8)	-0.0014 (8)	-0.0010 (8)
C26	0.0342 (10)	0.0336 (10)	0.0381 (11)	-0.0068 (8)	-0.0023 (9)	-0.0014 (8)
C27	0.0338 (10)	0.0333 (10)	0.0443 (11)	-0.0068 (8)	-0.0022 (9)	-0.0027 (9)
C28	0.0423 (12)	0.0397 (11)	0.0480 (12)	-0.0102 (10)	-0.0053 (10)	-0.0034 (9)
C29	0.0436 (12)	0.0427 (12)	0.0649 (15)	-0.0125 (10)	-0.0094 (11)	-0.0077 (11)

Geometric parameters (\AA , $^{\circ}$)

O1—C7	1.227 (2)	C14—H14B	0.9900
N1—C7	1.382 (2)	C15—C16	1.520 (3)
N1—C6	1.399 (2)	C15—H15A	0.9900
N1—C8	1.457 (2)	C15—H15B	0.9900
N2—C7	1.381 (2)	C16—C17	1.524 (3)
N2—C1	1.391 (2)	C16—H16A	0.9900
N2—C19	1.448 (2)	C16—H16B	0.9900
N3—N4	1.342 (2)	C17—C18	1.515 (3)
N3—C10	1.344 (2)	C17—H17A	0.9900
N3—C11	1.459 (2)	C17—H17B	0.9900
N4—N5	1.317 (2)	C18—H18A	0.9800
N5—C9	1.356 (2)	C18—H18B	0.9800
N6—N7	1.337 (2)	C18—H18C	0.9800
N6—C21	1.346 (2)	C19—C20	1.498 (2)
N6—C22	1.463 (2)	C19—H19A	0.9900
N7—N8	1.319 (2)	C19—H19B	0.9900
N8—C20	1.351 (2)	C20—C21	1.369 (2)
C1—C2	1.387 (2)	C21—H21	0.9500
C1—C6	1.399 (2)	C22—C23	1.523 (3)
C2—C3	1.392 (3)	C22—H22A	0.9900
C2—H2	0.9500	C22—H22B	0.9900
C3—C4	1.385 (3)	C23—C24	1.519 (2)
C3—H3	0.9500	C23—H23A	0.9900
C4—C5	1.399 (3)	C23—H23B	0.9900
C4—H4	0.9500	C24—C25	1.525 (3)
C5—C6	1.377 (3)	C24—H24A	0.9900
C5—H5	0.9500	C24—H24B	0.9900
C8—C9	1.496 (3)	C25—C26	1.523 (3)
C8—H8A	0.9900	C25—H25A	0.9900
C8—H8B	0.9900	C25—H25B	0.9900
C9—C10	1.373 (2)	C26—C27	1.524 (3)
C10—H10	0.9500	C26—H26A	0.9900
C11—C12	1.512 (3)	C26—H26B	0.9900
C11—H11A	0.9900	C27—C28	1.519 (3)
C11—H11B	0.9900	C27—H27A	0.9900
C12—C13	1.524 (3)	C27—H27B	0.9900
C12—H12A	0.9900	C28—C29	1.518 (3)
C12—H12B	0.9900	C28—H28A	0.9900
C13—C14	1.522 (3)	C28—H28B	0.9900
C13—H13A	0.9900	C29—H29A	0.9800
C13—H13B	0.9900	C29—H29B	0.9800
C14—C15	1.522 (2)	C29—H29C	0.9800
C14—H14A	0.9900		
C7—N1—C6	109.97 (14)	C15—C16—C17	114.31 (17)
C7—N1—C8	123.91 (14)	C15—C16—H16A	108.7

C6—N1—C8	126.02 (14)	C17—C16—H16A	108.7
C7—N2—C1	110.01 (14)	C15—C16—H16B	108.7
C7—N2—C19	122.99 (15)	C17—C16—H16B	108.7
C1—N2—C19	126.99 (15)	H16A—C16—H16B	107.6
N4—N3—C10	111.05 (15)	C18—C17—C16	113.09 (17)
N4—N3—C11	120.59 (15)	C18—C17—H17A	109.0
C10—N3—C11	128.28 (15)	C16—C17—H17A	109.0
N5—N4—N3	106.89 (14)	C18—C17—H17B	109.0
N4—N5—C9	109.21 (15)	C16—C17—H17B	109.0
N7—N6—C21	110.88 (14)	H17A—C17—H17B	107.8
N7—N6—C22	119.89 (14)	C17—C18—H18A	109.5
C21—N6—C22	129.19 (15)	C17—C18—H18B	109.5
N8—N7—N6	107.11 (15)	H18A—C18—H18B	109.5
N7—N8—C20	108.94 (15)	C17—C18—H18C	109.5
C2—C1—N2	131.37 (18)	H18A—C18—H18C	109.5
C2—C1—C6	121.48 (17)	H18B—C18—H18C	109.5
N2—C1—C6	107.15 (15)	N2—C19—C20	112.93 (14)
C1—C2—C3	116.63 (18)	N2—C19—H19A	109.0
C1—C2—H2	121.7	C20—C19—H19A	109.0
C3—C2—H2	121.7	N2—C19—H19B	109.0
C4—C3—C2	121.84 (17)	C20—C19—H19B	109.0
C4—C3—H3	119.1	H19A—C19—H19B	107.8
C2—C3—H3	119.1	N8—C20—C21	108.28 (16)
C3—C4—C5	121.48 (18)	N8—C20—C19	120.19 (15)
C3—C4—H4	119.3	C21—C20—C19	131.51 (16)
C5—C4—H4	119.3	N6—C21—C20	104.79 (15)
C6—C5—C4	116.72 (18)	N6—C21—H21	127.6
C6—C5—H5	121.6	C20—C21—H21	127.6
C4—C5—H5	121.6	N6—C22—C23	112.32 (14)
C5—C6—N1	131.52 (16)	N6—C22—H22A	109.1
C5—C6—C1	121.85 (16)	C23—C22—H22A	109.1
N1—C6—C1	106.63 (15)	N6—C22—H22B	109.1
O1—C7—N2	126.84 (16)	C23—C22—H22B	109.1
O1—C7—N1	126.95 (16)	H22A—C22—H22B	107.9
N2—C7—N1	106.20 (14)	C24—C23—C22	110.72 (15)
N1—C8—C9	112.95 (15)	C24—C23—H23A	109.5
N1—C8—H8A	109.0	C22—C23—H23A	109.5
C9—C8—H8A	109.0	C24—C23—H23B	109.5
N1—C8—H8B	109.0	C22—C23—H23B	109.5
C9—C8—H8B	109.0	H23A—C23—H23B	108.1
H8A—C8—H8B	107.8	C23—C24—C25	113.69 (15)
N5—C9—C10	108.03 (16)	C23—C24—H24A	108.8
N5—C9—C8	121.92 (16)	C25—C24—H24A	108.8
C10—C9—C8	130.05 (16)	C23—C24—H24B	108.8
N3—C10—C9	104.82 (15)	C25—C24—H24B	108.8
N3—C10—H10	127.6	H24A—C24—H24B	107.7
C9—C10—H10	127.6	C26—C25—C24	112.51 (16)
N3—C11—C12	112.22 (15)	C26—C25—H25A	109.1

N3—C11—H11A	109.2	C24—C25—H25A	109.1
C12—C11—H11A	109.2	C26—C25—H25B	109.1
N3—C11—H11B	109.2	C24—C25—H25B	109.1
C12—C11—H11B	109.2	H25A—C25—H25B	107.8
H11A—C11—H11B	107.9	C25—C26—C27	114.60 (17)
C11—C12—C13	112.66 (15)	C25—C26—H26A	108.6
C11—C12—H12A	109.1	C27—C26—H26A	108.6
C13—C12—H12A	109.1	C25—C26—H26B	108.6
C11—C12—H12B	109.1	C27—C26—H26B	108.6
C13—C12—H12B	109.1	H26A—C26—H26B	107.6
H12A—C12—H12B	107.8	C28—C27—C26	112.76 (17)
C14—C13—C12	112.57 (15)	C28—C27—H27A	109.0
C14—C13—H13A	109.1	C26—C27—H27A	109.0
C12—C13—H13A	109.1	C28—C27—H27B	109.0
C14—C13—H13B	109.1	C26—C27—H27B	109.0
C12—C13—H13B	109.1	H27A—C27—H27B	107.8
H13A—C13—H13B	107.8	C29—C28—C27	113.62 (19)
C13—C14—C15	114.46 (15)	C29—C28—H28A	108.8
C13—C14—H14A	108.6	C27—C28—H28A	108.8
C15—C14—H14A	108.6	C29—C28—H28B	108.8
C13—C14—H14B	108.6	C27—C28—H28B	108.8
C15—C14—H14B	108.6	H28A—C28—H28B	107.7
H14A—C14—H14B	107.6	C28—C29—H29A	109.5
C16—C15—C14	113.30 (16)	C28—C29—H29B	109.5
C16—C15—H15A	108.9	H29A—C29—H29B	109.5
C14—C15—H15A	108.9	C28—C29—H29C	109.5
C16—C15—H15B	108.9	H29A—C29—H29C	109.5
C14—C15—H15B	108.9	H29B—C29—H29C	109.5
H15A—C15—H15B	107.7		
C10—N3—N4—N5	0.6 (2)	N4—N5—C9—C10	0.3 (2)
C11—N3—N4—N5	177.67 (15)	N4—N5—C9—C8	-179.02 (16)
N3—N4—N5—C9	-0.6 (2)	N1—C8—C9—N5	-113.96 (19)
C21—N6—N7—N8	-0.7 (2)	N1—C8—C9—C10	66.8 (2)
C22—N6—N7—N8	177.02 (16)	N4—N3—C10—C9	-0.4 (2)
N6—N7—N8—C20	0.2 (2)	C11—N3—C10—C9	-177.17 (17)
C7—N2—C1—C2	-178.80 (18)	N5—C9—C10—N3	0.0 (2)
C19—N2—C1—C2	0.0 (3)	C8—C9—C10—N3	179.31 (18)
C7—N2—C1—C6	1.31 (19)	N4—N3—C11—C12	-107.0 (2)
C19—N2—C1—C6	-179.84 (15)	C10—N3—C11—C12	69.6 (2)
N2—C1—C2—C3	-179.77 (18)	N3—C11—C12—C13	-177.95 (16)
C6—C1—C2—C3	0.1 (3)	C11—C12—C13—C14	169.67 (17)
C1—C2—C3—C4	0.0 (3)	C12—C13—C14—C15	178.35 (16)
C2—C3—C4—C5	-0.5 (3)	C13—C14—C15—C16	175.90 (17)
C3—C4—C5—C6	0.9 (3)	C14—C15—C16—C17	-179.27 (17)
C4—C5—C6—N1	179.66 (17)	C15—C16—C17—C18	176.78 (18)
C4—C5—C6—C1	-0.7 (3)	C7—N2—C19—C20	-88.9 (2)
C7—N1—C6—C5	178.61 (18)	C1—N2—C19—C20	92.4 (2)

C8—N1—C6—C5	-4.8 (3)	N7—N8—C20—C21	0.3 (2)
C7—N1—C6—C1	-1.08 (18)	N7—N8—C20—C19	178.80 (16)
C8—N1—C6—C1	175.52 (16)	N2—C19—C20—N8	159.08 (17)
C2—C1—C6—C5	0.2 (3)	N2—C19—C20—C21	-22.8 (3)
N2—C1—C6—C5	-179.86 (15)	N7—N6—C21—C20	0.8 (2)
C2—C1—C6—N1	179.96 (16)	C22—N6—C21—C20	-176.61 (16)
N2—C1—C6—N1	-0.14 (18)	N8—C20—C21—N6	-0.6 (2)
C1—N2—C7—O1	177.12 (17)	C19—C20—C21—N6	-178.96 (17)
C19—N2—C7—O1	-1.8 (3)	N7—N6—C22—C23	-106.9 (2)
C1—N2—C7—N1	-1.95 (18)	C21—N6—C22—C23	70.3 (2)
C19—N2—C7—N1	179.15 (14)	N6—C22—C23—C24	177.04 (15)
C6—N1—C7—O1	-177.20 (17)	C22—C23—C24—C25	168.59 (16)
C8—N1—C7—O1	6.1 (3)	C23—C24—C25—C26	-178.67 (17)
C6—N1—C7—N2	1.86 (18)	C24—C25—C26—C27	177.38 (17)
C8—N1—C7—N2	-174.83 (15)	C25—C26—C27—C28	-178.60 (18)
C7—N1—C8—C9	-113.03 (18)	C26—C27—C28—C29	179.6 (2)
C6—N1—C8—C9	70.8 (2)		

Hydrogen-bond geometry (\AA , $^\circ$)

Cg2 is the centroid of the N3—N5/C9/C10 ring.

D—H···A	D—H	H···A	D···A	D—H···A
C2—H2···O1 ⁱ	0.95	2.59	3.502 (2)	162
C10—H10···N5 ⁱⁱ	0.95	2.44	3.317 (2)	153
C19—H19A···O1 ⁱ	0.99	2.43	3.334 (2)	152
C21—H21···N8 ⁱⁱⁱ	0.95	2.62	3.372 (2)	137
C22—H22A···Cg2 ^{iv}	0.99	2.89	3.664 (2)	135

Symmetry codes: (i) $-x+1, y-1/2, -z+1$; (ii) $x-1, y, z$; (iii) $x+1, y, z$; (iv) $-x+2, y-1/2, -z+1$.*Comparison of the selected (X-ray and DFT) geometric data (\AA , $^\circ$)*

Bonds/angles	X-ray	B3LYP/6-311G(d,p)
O1—C7	1.227 (2)	1.2256
N1—C7	1.382 (2)	1.3862
N1—C6	1.399 (2)	1.3954
N1—C8	1.457 (2)	1.4529
N2—C7	1.381 (2)	1.3838
N2—C1	1.391 (2)	1.3957
N3—N4	1.342 (2)	1.3447
N4—N5	1.317 (2)	1.3118
N4—N3—C10	111.05 (15)	111.56
N4—N3—C11	120.59 (15)	120.32
C10—N3—C11	128.28 (15)	128.09
N5—N4—N3	106.89 (14)	106.96
N4—N5—C9	109.21 (15)	109.85

Calculated energies.

Molecular Energy (a.u.) (eV)	Compound (I)
Total Energy TE (eV)	-44752.35
E_{HOMO} (eV)	-5.72
E_{LUMO} (eV)	-0.68
Gap ΔE (eV)	5.04
Dipole moment μ (Debye)	3.96
Ionisation potential I (eV)	5.72
Electron affinity A	0.68
Electronegativity χ	3.202
Hardness η	2.19
Softness σ	0.19
Electrophilicity index ω	2,03
